

Thermoelectric Properties and Crystal Structures of Au doped SiC/Si Composites

K.Nagasawa¹, H.Nakatsugawa¹, Y.Okamoto²

- 1- Graduate School of Engineering, Yokohama National University, 79-5 Tokiwadai, Hodogaya Ward, Yokohama, Kanagawa 240-8501, Japan
 - 2- Department of Material Science and Engineering, National Defense Academy, 1-10-20 Hashirimizu, Yokosuka, Kanagawa 239-8686, Japan
- Contact author: d07sb402@ynu.ac.jp

Abstract

SiC/Si/Au composites with polysilastyrene (PSS) additive as the sintering aids have been investigated the thermoelectric properties and crystalline characteristics for application of “Peltier Self-Cooling Semiconductor Device”. We decided the composition of SiC/Si/Au system showing high power factor, furthermore Hall coefficient measurements at room temperature revealed that the increase of electrical conductivity originated the rise of mobility. Scanning electron microscope observations confirmed the grain growth by virtue of Si additive. Elemental distributions in order of micro scale were cleared by electron probe micro analyzer. High temperature XRD measurement revealed that the appearance of marginal peaks occurred as the rise of temperature for 1173K.

Introduction

Silicon semiconductor devices have been progressed efficiency with gain of developed power. One of the most considerable problems interfering the development is that their devices are not capable of conduct an electric current of the spec owing to Joule heating. Yamaguchi, *et.al* [1][2] suggested new cooling system using of the Peltier material plate named “Self-Cooling Semiconductor Device”. This technology carries out the Peltier cooling with the use of flowing current in silicon power device (e.g PowerMOSFET, IGBT) itself by using of thermoelectric material instead of copper electrode in silicon power devices.

Thermoelectric properties of this applicable material are demanded the higher electrical conductivity, thermal conductivity and seebeck coefficient different from conventional thermoelectric material. Silicon carbide has considerable promise as the Self-Cooling Device material since it takes advantage of these desirable properties.

Recent studies of the physical properties for additional silicon carbide have been reported [3][4]. Moreover, many additional data have been reported the additional SiC thermoelectric materials, such as C [5,6], B₄C [7], Al [8], Ni [9].

As we know, SiC has a multitude of polytypes in more than 200 different structures. The most widely used is 3C, 4H and 6H type [10][11][12]. Recent study of the electrical conductivity of SiC semiconductor, which is the remarkable property in this work, indicates that single crystal and polycrystalline sample shows about $7.7 \times 10^2 \Omega\text{m}^{-1}$ [13] and $6.7 \times 10^2 \Omega\text{m}^{-1}$ [14] at room temperature respectively. Besides, co-worker has reported that the electrical conductivity of the 40% Si doped polycrystalline SiC shows $2.5 \times 10^3 \Omega\text{m}^{-1}$ at room temperature [15].

Heretofore, although many attempts to the additional SiC were devoted, to our knowledge, SiC sintered with Au additive has not been investigated in detail. The purpose of this study is to investigate the thermoelectric properties and crystal structure for SiC/Si/Au composite in order to apply the Self-Cooling Semiconductor Device.

Experimental procedure

Polycrystalline samples were prepared under the following condition by a conventional solid-state reaction. β -SiC, Si and Au powder were used as starting material, and polysilastyrene(PSS) were mixed as sintering aids. The mixing powder were formed pellet type by uniaxial pressing at $1 \times 10^6 \text{kg/m}^2$. Furthermore, the pellets were conducted the cold isostatic pressing at $3.5 \times 10^7 \text{kg/m}^2$. Their samples were sintered for 120min at 2373K in argon gas.

The measurement of electrical conductivity and Seebeck coefficient was performed ranging from 80 to 385K, and Hall coefficient was carried out at room temperature. The microstructures of the samples were observed using a scanning electron microscope on the fractured surface. The elementary distributions of Si, C and Au in microstructure were determined using the electron probe micro analyzer for polished surface of the samples. The crystal structure and phase of the samples were studied by powder X-ray diffractometry using $\text{CuK}\alpha$ radiation.

Results and discussion

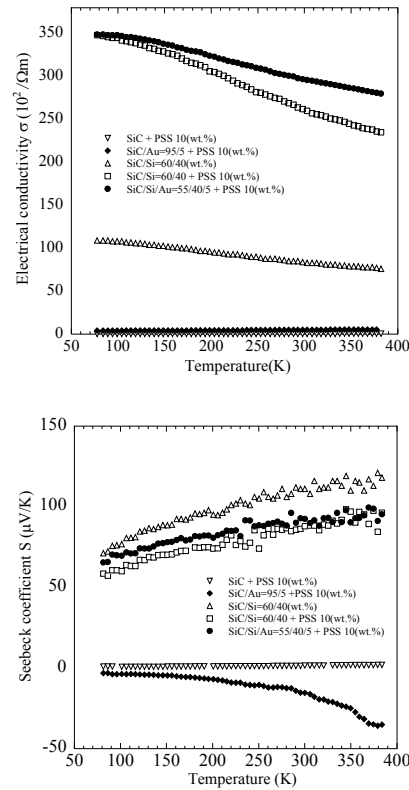
The temperature dependence of the electrical conductivity σ is shown in Fig. 1. At room temperature, the value of σ of PSS 10wt.% additive SiC/Si/Au=55/40/5wt.% was 3.5 times ($2.97 \times 10^4 / \Omega\text{m}$) as large as that of SiC/Si=60/40wt.% and this composition exhibited the maximum value of all samples. Si additive and non-additive samples showed a metallic and semiconductor behavior respectively in the temperature range of 80 to 385K.

Fig. 2 shows the temperature dependence of the Seebeck coefficient. PSS 10wt.% additive SiC/Si=95/5wt.% showed only negative S value. A maximum value of S in the range of all temperature occurs with SiC/Si=60/40wt.% sample, and at room temperature, it reached a value of approximately $111 \mu\text{V/K}$.

Table 1 shows the sample density, electrical transport properties, power factor $S^2\sigma$ and thermal conductivity κ at room temperature. The rise of sample density

results in an increase of mobility, and hence it causes an increase of electrical conductivity. Conclusively, it is seen that a maximum value of power factor $S^2\sigma$ at room temperature is the peak in the composite of PSS 10wt.% additive SiC/Si/Au=55/40/5wt.%, and reaching a value of $2.54 \times 10^{-4} \text{W/mK}^2$. Furthermore, same sample showed the high κ value relatively.

Fig. 1. Temperature dependence of electrical



| | SiC/Si=60/40 (wt.%) | SiC/Si=60/40 +PSS 10 (wt.%) | SiC/Si/Au=55/40/5 +PSS 10 (wt.%) |
|---|---------------------|-----------------------------|----------------------------------|
| σ ($10^2/\Omega\text{m}$) | 84.0 | 262 | 297 |
| R_H ($10^{-8}\text{m}^3/\text{C}$) | 3.09 | 1.99 | 1.93 |
| n ($10^{26}/\text{m}^3$) | 2.02 | 3.13 | 3.23 |
| μ ($10^4\text{m}^2/\text{Vs}$) | 2.60 | 5.21 | 5.73 |
| S (10^{-6}V/K) | 111 | 88.0 | 92.4 |
| $S^2\sigma$ (10^{-4}W/mK^2) | 1.03 | 2.03 | 2.54 |
| α ($10^{-5}\text{m}^2/\text{s}$) | 3.17 | 3.79 | 3.67 |
| d (10^3kg/m^3) | 1.69 | 2.10 | 2.17 |
| c (10^3J/kgK) | 0.684 | 0.675 | 0.658 |
| κ (W/mK) | 36.6 | 53.7 | 52.4 |

conductivity σ .

Fig. 2. Temperature dependence of Seebeck coefficient S.

Table 1. Electrical conductivity σ , Hall coefficient R_H , carrier concentration n , Hall mobility μ , Seebeck coefficient S, Power factor $S^2\sigma$, Thermal diffusivity α , Sample density d , Specific heat c and Thermal conductivity κ at room temperature.

Microstructure variation with varying composition ratio is shown in Fig. 3. When the Si and (or) PSS additive samples (b), (c) and (d) are compared to (a), it appears that SiC grain growth is developed and porosity is diminished. PSS above 10wt.% or Au additive sample was observed an increase of porosity. It follows that PSS above 10wt.% or Au additive tend to depress the grain growth. It can be explained that a mass of PSS additive (above 10wt.%) have a little influence on accelerating of high density but strong volume affect, and optimum amount of PSS additive is 10wt.%.

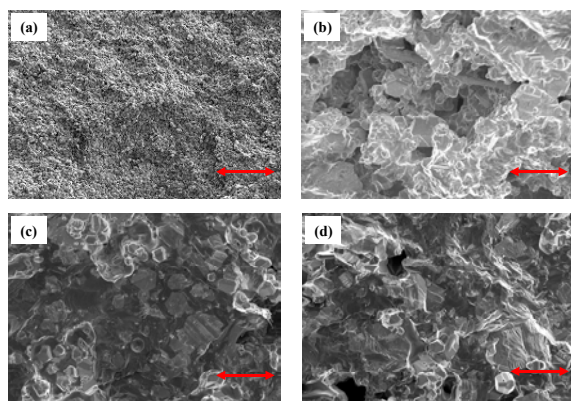
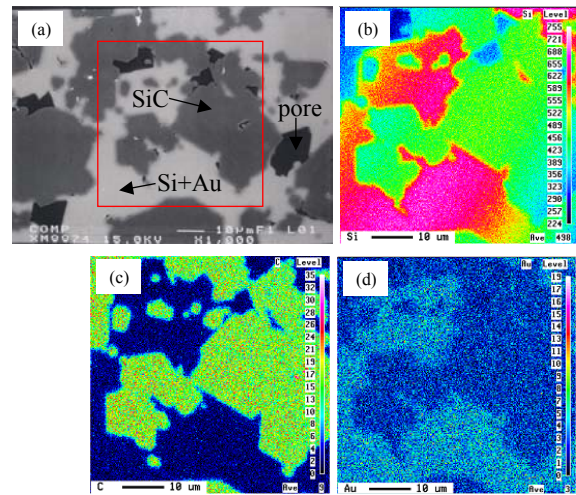


Fig. 3. SEM micrographs of fracture surface of (a)SiC/Au=95/5+PSS10(wt.%) (b)SiC/Si=60/40(wt.%) (c)SiC/Si=60/40+PSS10(wt.%) (d)SiC/Si/Au=55/40/5+PSS10(wt.%).

To investigate the elementary distribution of Si, C and Au in microstructure, we carried out the electron probe micro analysis for polished surface of the samples. Fig. 4 shows the backscatter electron images and the elementary distributions of Si, C and Au in PSS 10wt.% additive SiC/Si/Au=55/40/5wt.%. In Fig. 4 (b) and (c), it is considered that carbon detector region is SiC grain region since it is detected silicon in same location. Moreover the other region is additional Si region, implying that SiC and additional Si regions respectively are separated distinctly. In Fig. 4 (d), aurum is distributed totally and equally in additional Si region and not in SiC region. Besides, no chemical reaction between Au and Si is indicated by XRD measurement peak pattern. We infer that additional Si and Au of liquid phase existed in the interflow

condition in the space between growing SiC grains at sintering process and then it changed into the solid phase at cooling process (a).

Fig. 4. (a) The Backscatter electron image and



[(b)-Si, (c)-C and (d)-Au] the element distribution image in SiC/Si/Au=55/40/5+PSS10(wt.%).

The powder X-ray measurement was carried out for all samples. X-ray diffraction pattern indicate the evaporation of PSS and no chemical reactions of each other compound in sintering process. The pure substance of SiC (no doping SiC) is known the phase transition from 3C-SiC to 6H-SiC at about 2273K. Fabricated SiC samples are shown the diffraction pattern of 3C-SiC phase despite of sintering at 2273K. We infer that this reason is due to the excessive additive of Si. Fig. 5 shows the temperature dependence of X-ray diffraction pattern. Although there find no significant structural changes, we find to appear the marginal diffraction peaks in the vicinity of $2\theta=36.5$ and 60.5° as the temperature rise to 1173K. We carried out the identification of this newly appearance peaks by determined their bragg reflection angles and there is a possibility that their peaks are 6H-SiC. Ordinary, in other peaks, diffraction intensity tends to decline as the temperature rise because of the crystalline degeneracy by thermal lattice vibration. However, diffraction peaks in $2\theta=36.5$ and 60.5° tend to augment of intensity as the temperature rise to 1173K and there observation to not the shifting from neighboring mighty peak.

Judging from the results so far obtained, the peak appearances in $2\theta=36.5$ and 60.5° as to temperature rise can be explained the second phase transition from 3C-SiC to 6H-SiC.

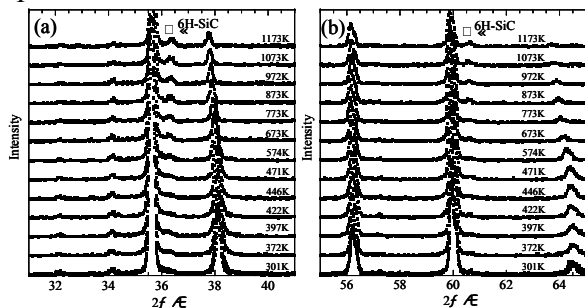


Fig. 5 Temperature dependence of XRD pattern of SiC/Si/Au=55/40/5+PSS10(wt%) (a) $2\theta=31-41^\circ$ (b) $2\theta=55-65^\circ$.

Conclusions

Si, Au and PSS additive β -SiC sintered semiconductor appears a maximum value of electrical conductivity and power factor at the composite of PSS 10wt.% additive SiC/Si/Au=55/40/5wt.%. It is considered that the high sample density and Au additive result in an increase of mobility, and hence lead to enhancement of electrical conductivity. Furthermore, SEM observation to investigate the trend of the high sample density exhibits that there is a peak of the grain growth at Si and PSS additive sample. In order to gain insight into the crystal characteristics of SiC/Si/Au composites, high temperature XRD carry out in the range of 300 to 1173K and confirm the appearance of the marginal diffraction peaks in the vicinity of $2\theta=36.5$ and 60.5° as the temperature rise. We conclude that the development of the peak is the second phase transition from 3C-SC as parent phase to 6H-SiC.

Acknowledgment

The Hall effect measurement system, scanning electron microscope and electron probe micro analyzer were used at the Instrumental Analysis Center in Yokohama National University. The high temperature XRD measurement was carried out at the School of Chemistry in University of Birmingham. This research was performed in the graduate school of engineering of

Yokohama National University during the tenure of a fellowship.

References

- [1] S. Yamaguchi, Y. Okamoto, A. Yamamoto and M. Hamabe, *Proc. 26th Int. Conf. Thermoelectrics*, O-G-1, (2007).
- [2] S. Yamaguchi, "Peltier cooling for Semiconductor Devices", *ULVAC* **52** (2007) pp.14-17 (Japanese).
- [3] S.B.Ma, Y.P.Sun, B.C.Zhao, P.Tong, X.B.Zhu and W.H.Song, *Physica B.* **394** (2007) 122.
- [4] Z.Huang and Q.Chen, *J. Magn. Magn. Mater.* **313** (2007) 111.
- [5] M.Fujisawa, T.Hata, P.Bronsveld, V.Castro, F.Tanaka, H.Kikuchi and Y.Imamura, *J. Eur. Ceram. Soc.* **25** (2005) 2735.
- [6] M.Fujisawa, T.Hata, H.Kitagawa, P.Bronsveld, Y.Suzuki, K.Hasezaki, Y.Noda and Y.Imamura, *Renew. Energ.* **33** (2008) 309
- [7] M.Uehara, R.Shiraishi, A.Nogami, N.Enomoto and J.Hojo, *J. Eur. Ceram. Soc.* **24** (2004) 409.
- [8] Y.Okamoto, A.Aruga, H.Tashiro, J.Morimoto and T.Miyakawa, *Proc. 14th Int. Conf. Thermoelectrics* (1995) 269.
- [9] Y.Okamoto, K.Kato, J.Morimoto and T.Miyakawa, *Proc. 16th Int. Conf. Thermoelectrics* (1997) 236.
- [10] L.L.Snead, T.Nozaawa, Y.Katoh, T.S.Byun, S.Kondo and D.A.Petty, *J. Nucl. Mater.* **371** (2007) 329.
- [11] M.S.Miao and W.L.Lambrech, *Phys. Rev. B* **68** (2003) 125204.
- [12] K.Irmscher, *Mater. Sci. Eng.* **B91** (2002) 358.
- [13] A.Kondo, *J. Ceram. Soc. Jpn.* **100** (1992) 1225.
- [14] K.Kato, K.Asai, Y.Okamoto, J.Morimoto and T.Miyakawa, *J. Mater. Res.* **14** (1999) 1752.
- [15] Y.Okamoto, H.Inai and J.Morimoto *J. Jpn. Soc. Powder and Powder Met* **45** (1998) 905.